A Technique to Determine Uplink Range Calibration Due to Charged Particles

S. C. Wu and F. B. Winn
Tracking Systems and Applications Section

A technique is presented to determine uplink range change due to line-of-sight charged particles using downlink S/X range and doppler and 2-way DRVID data. The line-of-sight relative *charged-particle distribution is first estimated from these data by a point-matching method. The uplink range change is then synthesized by the weighted sum of the delayed downlink range changes. Simulation analysis shows 2 to 6 cm agreement between the "true" and the synthesized uplink range changes. Demonstration using Viking 1975 radio metric data shows 4 to 22 cm consistency between the uplink range calibration solutions synthesized from S-DRVID and X-DRVID. The consistency is an order of magnitude superior to that equating uplink and downlink effects.*

I. Introduction

During the previous interplanetary missions (including Viking '75) there have been no requirements for the calibration of the range change due to charged-particle effects. These effects are calibrated only for the doppler. For interplanetary tracking over ~10 A.U. (e.g., Voyager '77) the range change due to charged particles also needs to be calibrated. This will require both uplink and downlink range calibrations.

The radio metric data currently available are S- and X-band DRVID (Ref. 1), S/X dual-frequency doppler and range (Ref. 2). The types of these data are summarized in Table 1. S-DRVID, despite being 2-way data, provides only relative range-change information. X-DRVID, containing S-band uplink and X-band downlink, also is a relative measurement. S/X doppler is a "cleaner" downlink measurement. Although it is a relative measurement as well, it can be fitted to S/X range data (downlink) to infer absolute range calibration due to charged-particle effects. The uplink range calibration, on the other hand, is still a problem to be solved. The determination of this quantity from the above radio metric data requires the knowledge of the line-of-sight charged-particle distribution.

Winn, et al. (Ref. 3) proposed a scheme to estimate the mean location of the charged-particle concentration along the line-of-sight under the assumptions that the charged-particle cloud is (1) singular, (2) discrete, and (3) fixed in space. The uplink calibration can then be inferred from the delayed downlink calibration. This calibration scheme is indeed an improvement over that equating uplink to downlink. However, the above three constraints limit its application.

In this article a technique is presented to determine uplink range calibration with the above first two constraints removed. This technique requires only that the line-of-sight *relative* distribution of the charged particles be fixed over a period of time. The line-of-sight is first divided into a finite number of segments. A set of constrained linear algebraic equations of the

relative charged-particle distribution is set up by a point-matching method (Ref. 4). The solution of this relative charged-particle distribution provides the weights with which the delayed downlink calibrations are summed to synthesize the desired uplink calibrations.

Simulation analysis shows that the synthesized uplink calibration has an accuracy of better than 6 cm for a 20-minute one-way light time. A 20-cm (1σ) noise is assumed for one of the two observables to simulate the DRVID noise (Table 1). Application to the Viking 1975 radio metric data is demonstrated. The uplink calibration solutions synthesized from S-DRVID and X-DRVID show a 4 to 22 cm agreement.

II. Formulation

In the following analysis it is assumed that 2-way S-band DRVID and downlink S/X doppler and range data are available. Figure 1 depicts the geometry of the spacecraft, the deep-space station, and the charged-particle cloud. Let the charged-particle *relative* distribution be $w(t')$ at a distance t' light-minutes away from the spacecraft along the line-of-sight. This distribution $w(t')$ will be assumed fixed over the whole pass. The *absolute* distribution of the charged particles at any time t is the product of $w(t')$ and a temporal function $p(t)$. The a priori knowledge of $p(t)$ is not needed as will be seen. The uplink and downlink range changes due to the charged particles can be written as

$$R_u(t) = \int_0^T w(t')\, p(t - T - t')\, dt' \tag{1}$$

and

$$R_d(t) = \int_0^T w(t')\, p(t - T + t')\, dt' \tag{2}$$

where T is the one-way light time, and t is measured at the DSS. It is understood that $w(t')$ is non-negative and normalized:

$$\int_0^T w(t')\, dt' = \int_0^T |w(t')| dt' = 1 \tag{3}$$

The equation relating the uplink and downlink range changes from Eqs. (1) and (2) would be too complicated to be practical. An approximation accurate enough for practical uses can be made on the following basis. Comparing Eqs. (1) and (2) we see that for each infinitesimal component of downlink $R_d(t)$ there corresponds an equal uplink component which will appear only at a time $2t'$ later as received by the DSS. Hence an approximate expression for $R_u(t)$ would be

$$R_u(t) = \int_0^T w(t')\, R_d(t - 2t')\, dt' \tag{4}$$

This expression contains no temporal function $p(t)$. The uplink range change $R_u(t)$ can be synthesized once the relative distribution $w(t')$ is determined.

Note that both $R_u(t)$ and $R_d(t)$ in Eq. (4) are *absolute* range changes. Since DRVID (2-way) and S/X doppler (downlink) provide only relative range changes it is desired to reduce Eq. (4) in terms of relative quantities. Let the absolute uplink and downlink range changes at t_0 be $R_u(t_0)$ and $R_d(t_0)$, respectively. Then Eq. (4) can be rewritten as

$$\begin{aligned} R_u(t_0) + f_u(t) &= \int_0^T w(t')\, [R_d(t_0) + f_d(t - 2t')]\, dt' \\ &= R_d(t_0) + \int_0^T w(t')\, f_d(t - 2t')\, dt' \end{aligned}$$

or

$$f_u(t) = \int_0^T w(t')\, f_d(t - 2t')\, dt' + R_d(t_0) - R_u(t_0) \tag{5}$$

where f_u and f_d are relative range changes with zero references at $t = t_0$. The existence of the quantity $R_d(t_0) - R_u(t_0)$ in this equation presents no difficulties in the solution of $w(t')$. Although this quantity can be eliminated by the substitution of Eq. (4) with $t = t_0$, it is desirable to retain it as an additional solve-for unknown to eliminate the effect of DRVID noise at t_0. Elimination of this term will result in a bias in $f_u(t)$ when DRVID data at t_0 is inaccurate; this, in turn, will deteriorate the solution of $w(t')$. It should be noted that $f_d(t)$ has to be available at least $2T$ prior to $f_u(t)$ for Eq. (5) to be valid.

A simple approach to solve Eq. (5) is that of point matching (Ref. 4). The line-of-sight is divided into N segments of equal lengths. Over each segment the distribution is considered to be uniform. Hence Eq. (5) is reduced into the following summation:

$$f_u(t) = \sum_{n=1}^{N} W_n \int_{(n-1)T/N}^{nT/N} f_d(t - 2t')\, dt' + R_{d-u}(t_0) \tag{6}$$

Here, $f_d(t)$ represents the downlink S/X doppler. The (relative) uplink $f_u(t)$ is obtained from the difference[1] of S-DRVID and S/X doppler.

The unknowns W_n, $n = 1, 2, \ldots, N$ and $R_{d-u}(t_0)$ can be solved by M ($> N + 1$) equations resulting from the substitution of M different values of t in Eq. (6) subjected to the constraints reduced from Eq. (3):

$$\frac{T}{N} \sum_{n=1}^{N} W_n = 1 \tag{7}$$

and

$$W_n \geqslant 0, n = 1, 2, \ldots, N. \tag{8}$$

A linear least-squares process with constraints (Ref. 5) can be applied to solve for the $N + 1$ unknowns.

Once the W_n are determined, the absolute uplink range change $R_u(t)$ can be synthesized in two steps: (1) the S/X doppler is fitted to the S/X range points to yield the absolute downlink $R_d(t)$, and (2) the uplink $R_u(t)$ is calculated by the reduced form of Eq. (4):

$$R_u(t) = \sum_{n=1}^{N} W_n \int_{(n-1)T/N}^{nT/N} R_d(t - 2t')\, dt' \tag{9}$$

III. Simulation Analysis

To illustrate the uplink range calibration technique a simulation analysis is given in this section. A temporal function $p(t)$ describing the line-of-sight charged-particle content is assumed to be that shown in Fig. 2. Also assumed are the three models of line-of-sight relative charged-particle distribution as shown in Fig. 3. Here a 20-min one-way light time between spacecraft and DSS is assumed. The first model contains a single plasma uniformly distributed over a distance of one light minute; the second contains a nonuniform plasma over 2 light minutes; and the third contains two discrete plasmas of different spreads and densities.

The simulated S/X doppler is calculated by Eq. (2) with the zero-reference set at $t_0 = 2T$. The simulated S-DRVID is calculated by summing Eqs. (1) and (2), also with $t_0 = 2T$ as zero reference. The DRVID noise is simulated by adding a gaussian noise of 0.2-m standard deviation. These simulated S/X doppler and DRVID are plotted in Fig. 4.

To reduce the effect of DRVID noise, the number of equations M is made larger than the number of unknowns $N + 1 = 21$. The solutions of W_n using $M = 60$ are shown in Fig. 5 for the three models. The assumed true distributions of Fig. 3 are redrawn for comparison. The computed distributions indeed display the plasma concentrations. The larger smeared effect in Model 3 is believed due to the error in Eq. (4) with widely spread distribution.

The synthesized uplink range changes from Eq. (9) and the combined 2-way range changes are plotted in Fig. 6. The true uplink, downlink, and 2-way range changes are also shown for comparison. The synthesized quantities are essentially indistinguishable from the corresponding true quantities. The 2-way range changes obtained by simply doubling the downlinks are inserted to show how much they deviate from the true and the synthesized solutions. Table 2 compares the RMS deviation between these solutions. Synthesized results for a reduced number of equations ($M = 40$) are also included to demonstrate the convergence of solutions with increasing M.

The computed W_n with $M = 40$ are plotted in Fig. 7. The synthesized range changes are essentially identical to those with $M = 60$ (Fig. 6). A comparison of Figs. 5 and 7 indicates that the range change can be accurately determined from a not-so-accurate spatial distribution. This is due to the fact that the former is a linear combination of the latter; a first-order approximation of the distribution provides a second-order approximation of the range change. Hence, detailed resolution of the line-of-sight spatial distribution is not needed in the synthesis of uplink range change. Resolution of the order of light minutes is considered appropriate.

IV. Viking 1975 Radio Metric Data Demonstration

This section provides a demonstration for the calibration technique through applying to the Viking '75 radio metric data. Since actual uplink range changes are not known, the accuracy is estimated by comparing the results from different sets of observables undergoing the same media effect. That is, the result determined from the correlation between S/X doppler and S-band DRVID can be compared with that from S/X doppler and X-band DRVID. Hence, only passes with both S- and X-DRVID available are to be selected for the demonstration. In the following eight passes from Viking B Orbiter are selected in which the first six are for SEP (Sun-Earth-probe angle) ~30 deg and the remaining two are for SEP ~8 deg (Fig. 8).

[1]Or, alternatively, from the difference of X-DRVID and $(3/11)^2$ times S/X doppler, where 3/11 is the ratio between downlink X- and S-band carriers.

Figure 9 displays the S/X doppler as fitted to the S/X range points. The square-wave distortion effect has been removed from each range point by adding the difference of the nearby S-DRVID mean and X-DRVID mean.[2] Spacecraft delay, station delay and Z-correction are not removed from these range points. Figure 10 displays the corresponding S- and X-DRVID data during these passes. S-DRVID appears to have less noise than X-DRVID.

Since the downlink S-band carrier frequency differs from that of uplink by a factor 240/221, f_d in Eq. (6) is now given by $(240/221)^2$ times S/X doppler; f_u, as before, is given by S-DRVID subtracted by S/X doppler or X-DRVID subtracted by $(3/11)^2$ of S/X doppler. Also, since the S/X doppler data in most passes are taken once per minute the line-of-sight is conveniently divided into cells one light minute long.

Figure 11 compares the synthesized 2-way (uplink and downlink) range changes using S-DRVID and using X-DRVID. The RMS difference is 4 to 22 cm. The larger discrepancy is due to either (1) charged-particles having weak second-order dynamic that the observables contain little information about its distribution, as in Fig. 11 (d), or (2) X-DRVID being too noisy, as in Fig. 11(b) (cf. Fig. 10(b)). In all cases the consistency is better than that between 2X downlink[3] (continuous lines in Fig. 11) and either of these synthesized 2-way range changes. Typically it is an order of magnitude better. Table 3 summarizes the statistic of the comparison.

It should be pointed out that on October 26 each X-DRVID point was taken 10 s after the corresponding S-DRVID point and that the synthesized range changes actually have a 10-s relative shift. The RMS difference in Fig. 11(g) would have been reduced if the same S/X doppler set had been used for both synthesized range changes. For the remaining seven passes the S-DRVID and X-DRVID were taken alternately at 1-minute intervals; once the relative charged-particle distributions were reconstructed, the synthesized range changes were calculated on the same time frame.

As an intermediate result, the line-of-sight relative charged-particle distribution is shown in Fig. 12. The distance between the spacecraft and DSS along the line-of-sight is ~20 light minutes for the first six passes (Fig. 12(a) to (f)), and is ~21 light minutes for the remaining two passes (Fig. 12(g) to (h)). For comparison, the mean plasma locations determined by the method of Ref. 3 are also included (shown as vertical arrows).

From Fig. 12 it is observed that the computed charged-particle distributions have a concentration near 13 to 14 light minutes from the spacecraft in most cases. This agrees with the nearest-to-Sun point on the line-of-sight which is 12.8 light minutes from the spacecraft, as depicted in Fig. 8, during these passes. The better consistency among the results using S-DRVID once again indicates lower S-DRVID noise.

It should be pointed out that the computed concentration is only for the varying component of the charged-particle cloud. The concentration of the stationary charged-particle cloud is left out of the solution. This however, will not degrade the range calibration accuracy since the location of the stationary charged-particle cloud is immaterial in the synthesis of uplink range from downlink.

V. Discussions

Uplink range calibration due to charged particles can be determined from current radio-metric data. One may simply equate the uplink effect to the downlink effect by using S/X doppler and range (both downlink only). Unless the charged-particle cloud is concentrated near the spacecraft or is stationary, the accuracy is considered to be poor. With the knowledge of the Sun-Earth-probe geometry, one can improve the accuracy by equating the uplink effect to the delayed downlink, the delay t' being twice the light time between the spacecraft and the nearest-to-Sun point on the line-of-sight. The accuracy can be further improved by the mean-plasma-location approach (Ref. 3) which determines the delay t' by correlating the S/X doppler to DRVID. As the charged-particle cloud spreads out along the line-of-sight over several light minutes, the accuracy of these solutions will deteriorate and one will have to rely on the synthesis approach to maintain good accuracy of uplink range calibration.

Two-way doppler, which is the time rate of change of 2-way range, is directly available from the synthesized 2-way range change. Although DRVID does provide this information, the inherent noise prevents its direct application before undergoing proper smoothing process. The smoothing process, however, will filter out any short-term charged-particle variation effects. The reduction of 2-way doppler from synthesized 2-way range requires no smoothing process and hence, will retain these short-term effects.

VI. Conclusions

A technique to determine uplink charged-particle range calibration has been presented. The charged-particle effect is synthesized by the solution of relative charged-particle distribution along the line-of-sight. Resolution of distribution is not stringent; resolution of the order of light minutes is appro-

[2]As proposed by T. Komarek of Telecommunication Systems Section, Jet Propulsion Laboratory.

[3]The 2X downlink has been shifted upward by a factor $[1 + (240/221)^2]/2$ to account for the lower uplink carrier frequency.

priate. Simulation analysis has shown an accuracy better than 6 cm for a 20-min one-way light time with a 20-cm (1σ) noise in the simulated DRVID data. Application to the Viking '75 radio-metric data has demonstrated a 4 to 22 cm consistency between the results synthesized from S-band DRVID and from X-band DRVID. The only constraint for this technique is the assumption that the line-of-sight *relative* distribution of the charged-particles be fixed over the pass.[4] This is not an unrealistic assumption considering the ~10 hours required for a solar plasma to move, at ~500 km/s speed (Ref. 6), over a distance of one light minute.

The line-of-sight charged-particle distribution is a by-product of the calibration technique. This information is valuable in the investigation of solar plasma activities. For a detailed solar-plasma spatial structure a more accurate expression would be required in place of Eq. (4). This is currently being studied.

[4]It is sufficient to assume such condition over a period ~3X the one-way light time between spacecraft and DSS.

References

1. MacDoran, P.F., "A First-Principles Derivation of the Differenced Range Versus Integrated Doppler (DRVID) Charged-Particle Calibration Method," *Space Programs Summary 37-62,* Vol. II, pp. 28-34, March 31, 1970.
2. Madrid, G.A., "The Measurement of Dispersive Effect Using the Mariner 10 S- and X-Band Spacecraft to Station Link," *DSN Progress Report 42-22,* pp. 22-27, August 15, 1974.
3. Winn, F.B., Wu, S.C., Komarek T., Lam, V.W., and Royden, H.N., "A Solar Plasma Stream Measured by DRVID and Dual Frequency Range and Doppler Radiometric Data," *DSN Progress Report 42-37,* pp. 43-54, Feb. 15, 1977.
4. Harrington, R.F., *Field Computation by Moment Methods,* Macmillan, 1968.
5. Lawson, C.L., and Hanson, R.J., *Solving Least Squares Problems,* Prentice Hall, Inc. 1974.
6. Snyder, C.W., Neugebauer, M., and Rao, U.R., "The Solar Wind Velocity and Its Correlation with Cosmic Ray Variations and with Solar and Geomagnetic Activity," *J. Geophys. Res.,* Vol. 68, p. 6361, 1963.

Table 1. Viking 1975 radio metric data

Data type	Uplink/downlink	Absolute/relative	Typical noise level
S-DRVID	2-way	Relative	0.2 m
X-DRVID	Uplink[a]	Relative	0.2 m
S/X doppler	Downlink	Relative	0.01 m
S/X range	Downlink	Absolute	0.2 m

[a]X-DRVID actually consists of uplink S-DRVID plus downlink X-DRVID that equals uplink S-DRVID with ~ 6% error

Table 2. RMS Deviation from "true" 2-way range—simulation

	Model 1	Model 2	Model 3
Synthesized 2-way (M = 60)	1.9 cm	3.4 cm	3.7 cm
Synthesized 2-way (M = 40)	3.4 cm	4.1 cm	5.8 cm
2 X downlink	75.7 cm	77.4 cm	65.8 cm

Table 3. Statistic of synthesized 2-way range changes—Viking '75 radio metric data

Pass	Date	DSS	Number of cells	Number of equations	Residual of equations (S)	Residual of equations (X)	Difference from 2X downlink (S)	Difference from 2X downlink (X)	(S) - (X)
(a)	8/16/76	43	20	31	0.49 m	0.55 m	0.39 m	0.34 m	0.08 m
(b)	8/16/76	63	20	26	0.32	0.50	0.41	0.20	0.22
(c)	8/22/76	63	20	38	0.28	0.58	1.17	1.17	0.04
(d)	9/23/76	63	20	46	0.24	0.51	1.14	0.95	0.22
(e)	8/24/76	63	20	22	0.23	0.35	0.88	0.77	0.11
(f)	8/25/76	63	20	36	0.16	0.46	1.12	1.16	0.07
(g)	10/26/76	43	21	50	0.52	0.82	2.61	2.61	0.20
(h)	11/01/76	43	21	30	0.51	0.55	1.48	1.56	0.17

(S) 2-way range change synthesized from S-DRVID

(X) 2-way range change synthesized from X-DRVID

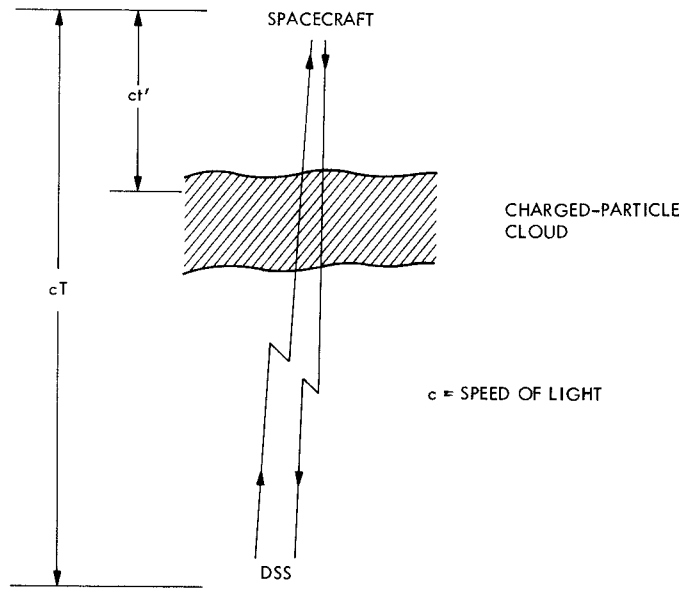

Fig. 1 Geometry of the problem

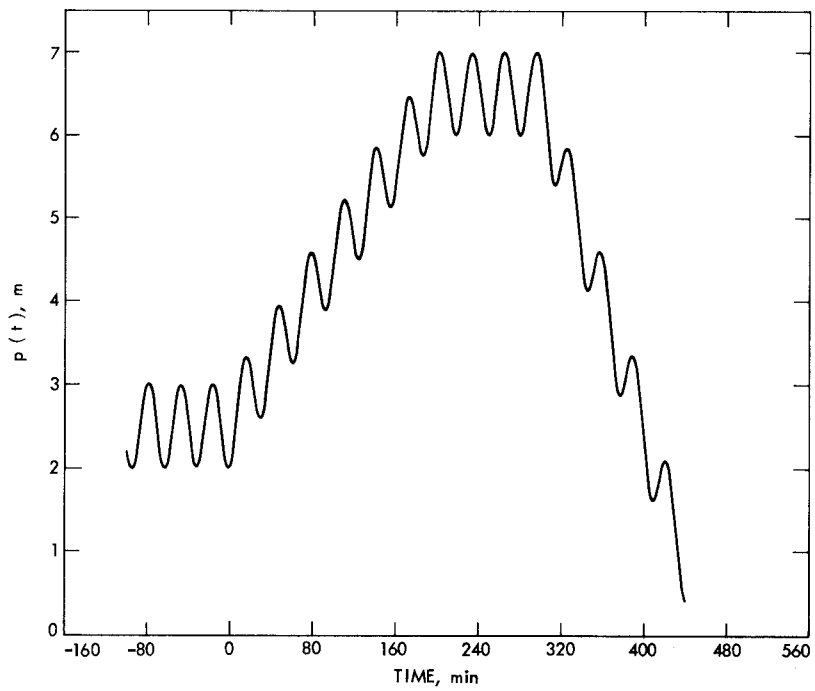

Fig. 2. Total line-of-sight charged-particle content (in terms of range change)

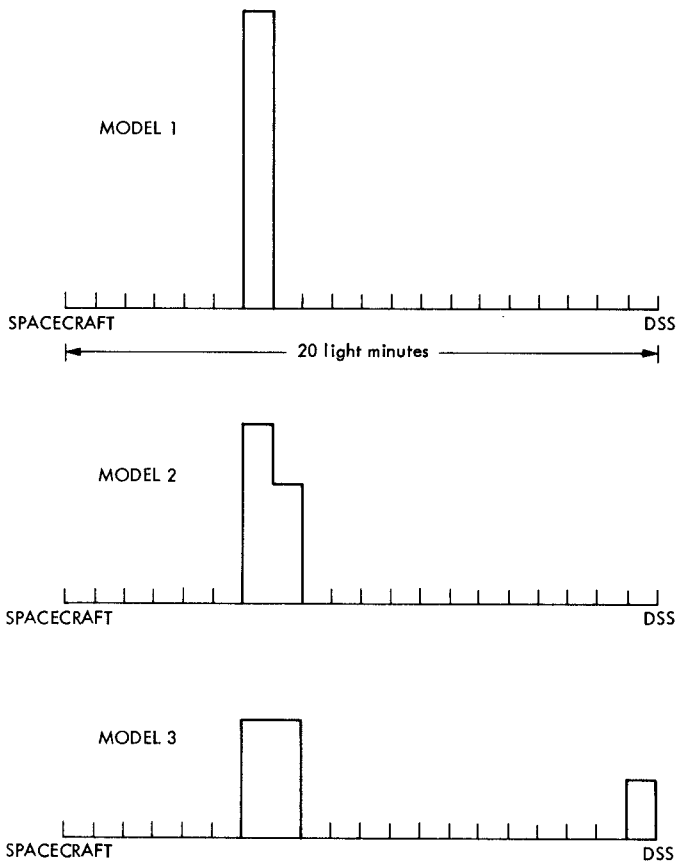

Fig. 3 Line-of-sight charged-particle relative distribution models

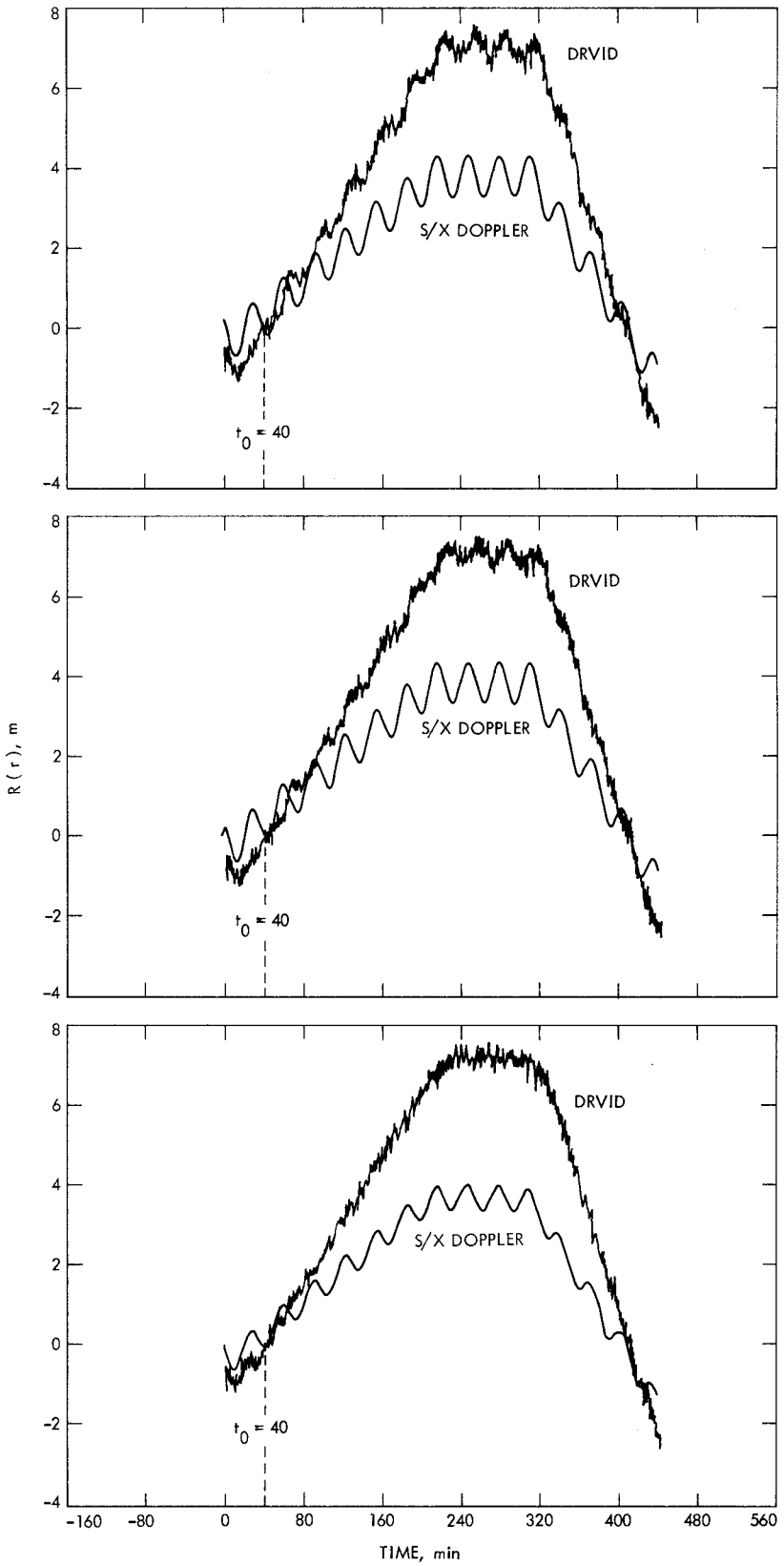

Fig. 4. Simulated DRVID and S/X band doppler (a) Model 1, (b) Model 2, (c) Model 3

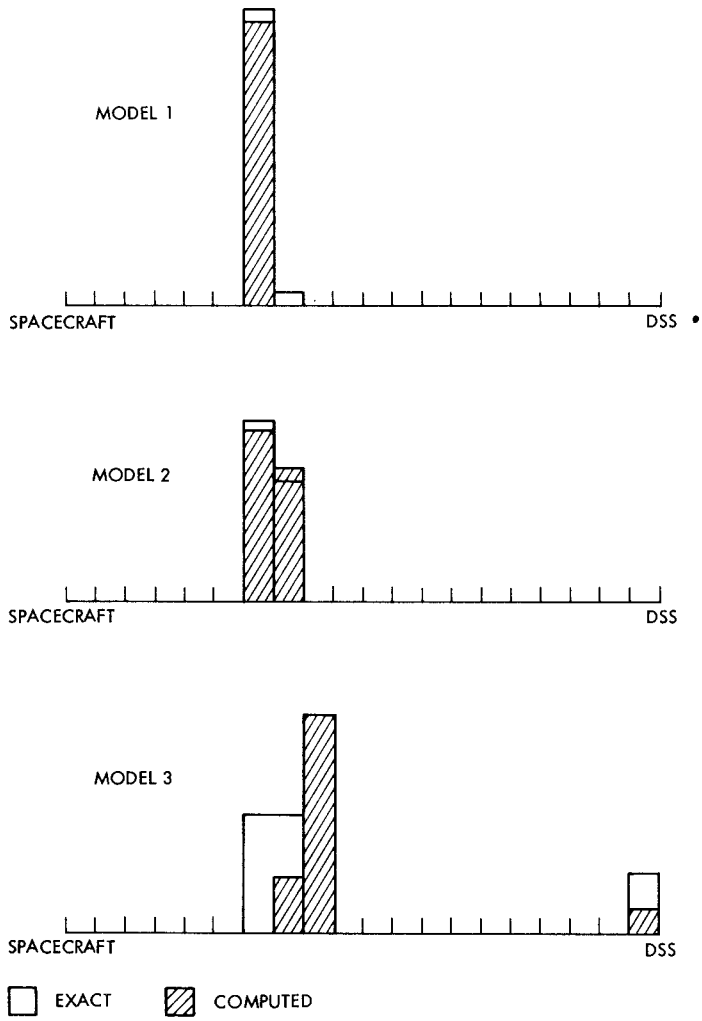

Fig. 5. Solutions of line-of-sight charged-particle relative distribution (M = 60)

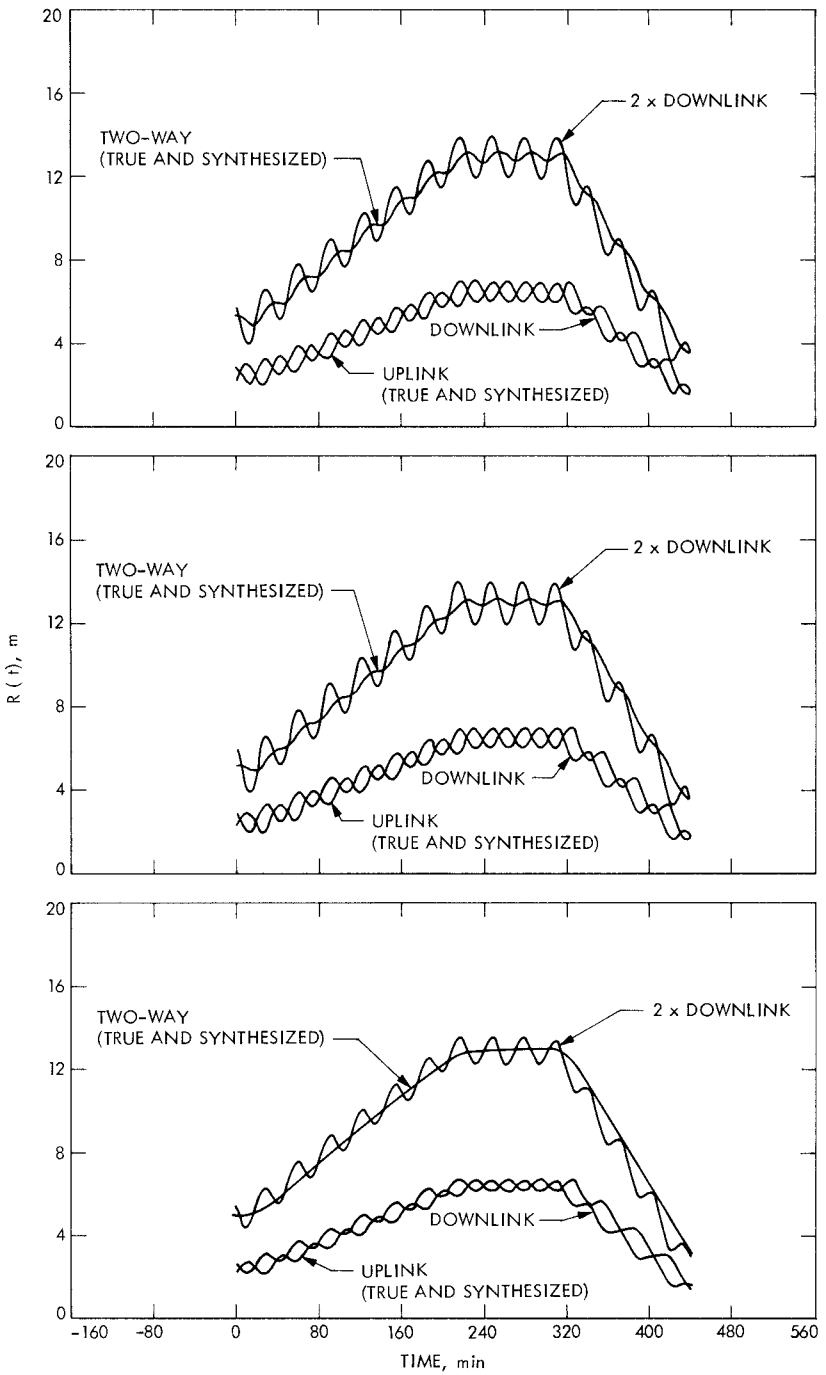

Fig. 6. Range changes due to charged particles (a) Model 1, (b) Model 2, (c) Model 3

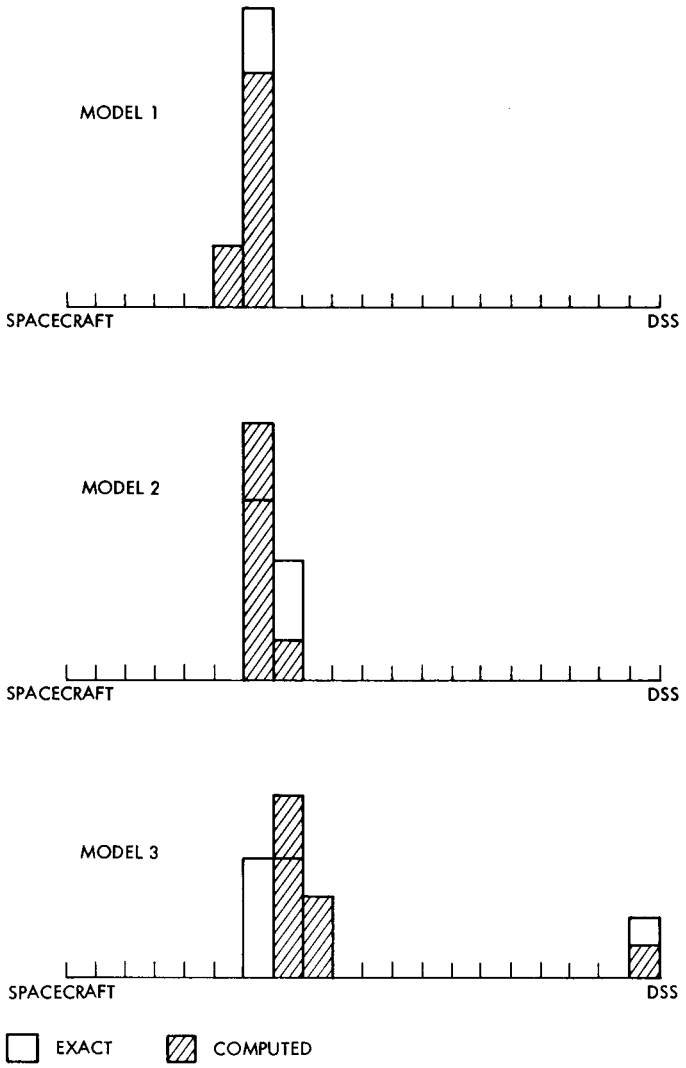

Fig. 7. Solutions of line-of-sight charged-particle relative distribution (M = 40)

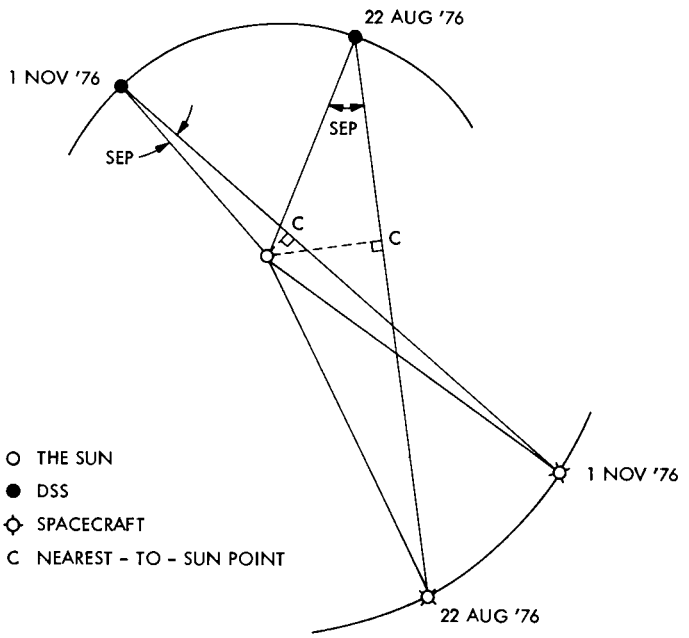

Fig. 8. Heliocentric geometry of deep space station and spacecraft (Viking B)

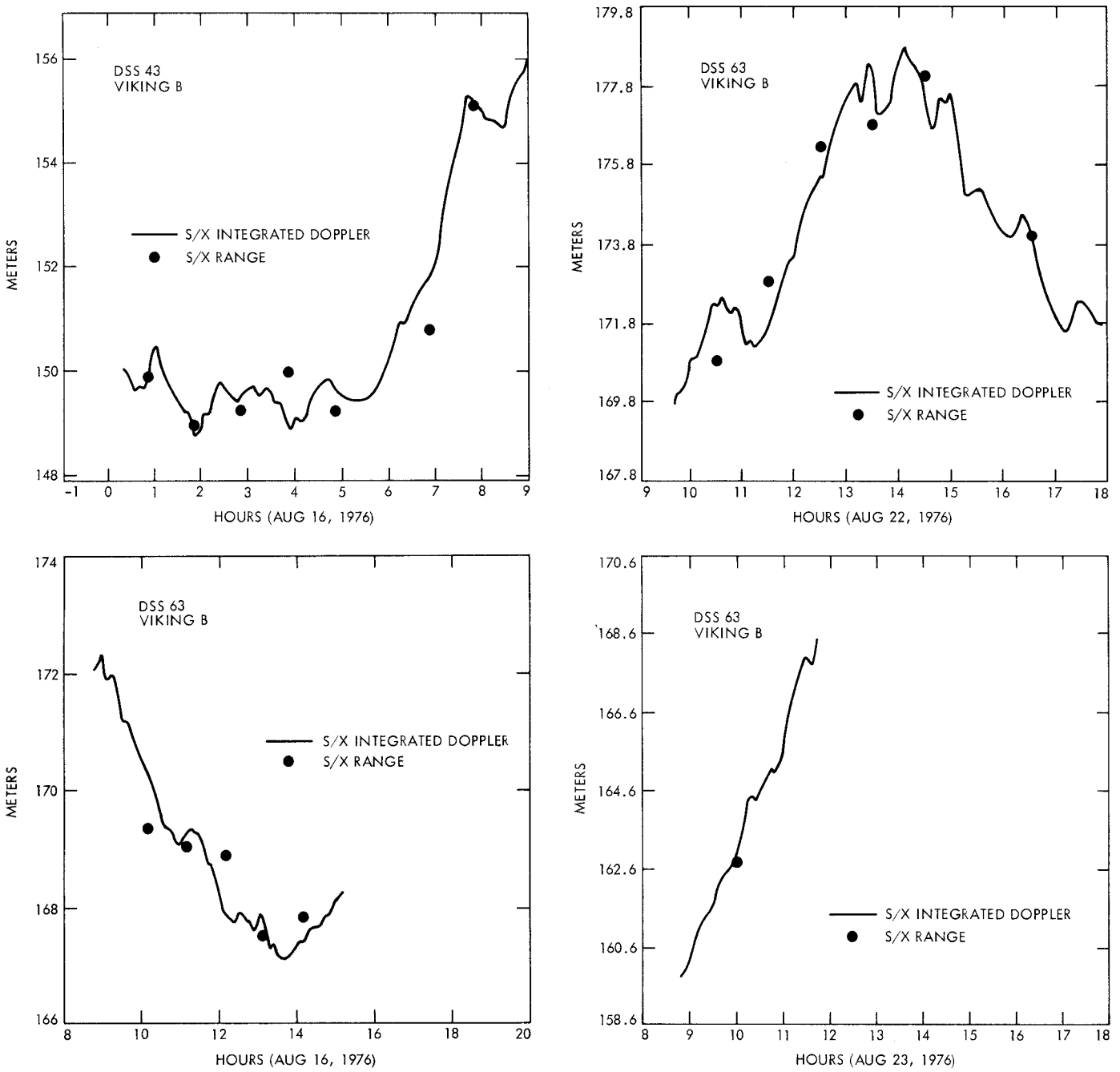

Fig. 9. S/X integrated doppler and S/X range

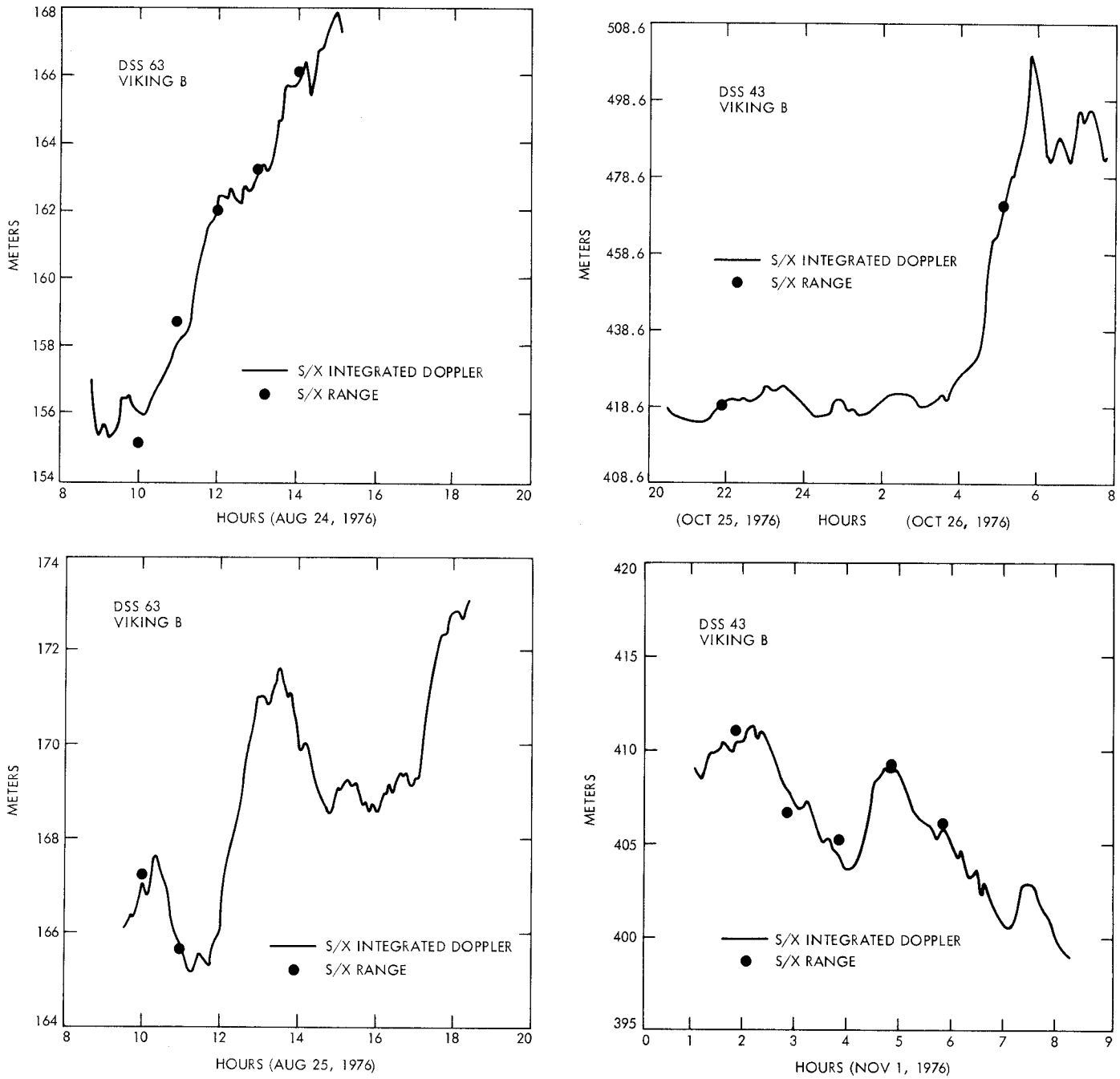
DSS 63
VIKING B
S/X INTEGRATED DOPPLER
S/X RANGE
METERS
HOURS (AUG 24, 1976)
DSS 43
VIKING B
S/X INTEGRATED DOPPLER
S/X RANGE
METERS
(OCT 25, 1976) HOURS (OCT 26, 1976)
DSS 63
VIKING B
S/X INTEGRATED DOPPLER
S/X RANGE
METERS
HOURS (AUG 25, 1976)
DSS 43
VIKING B
S/X INTEGRATED DOPPLER
S/X RANGE
METERS
HOURS (NOV 1, 1976)

Fig. 9 (contd)

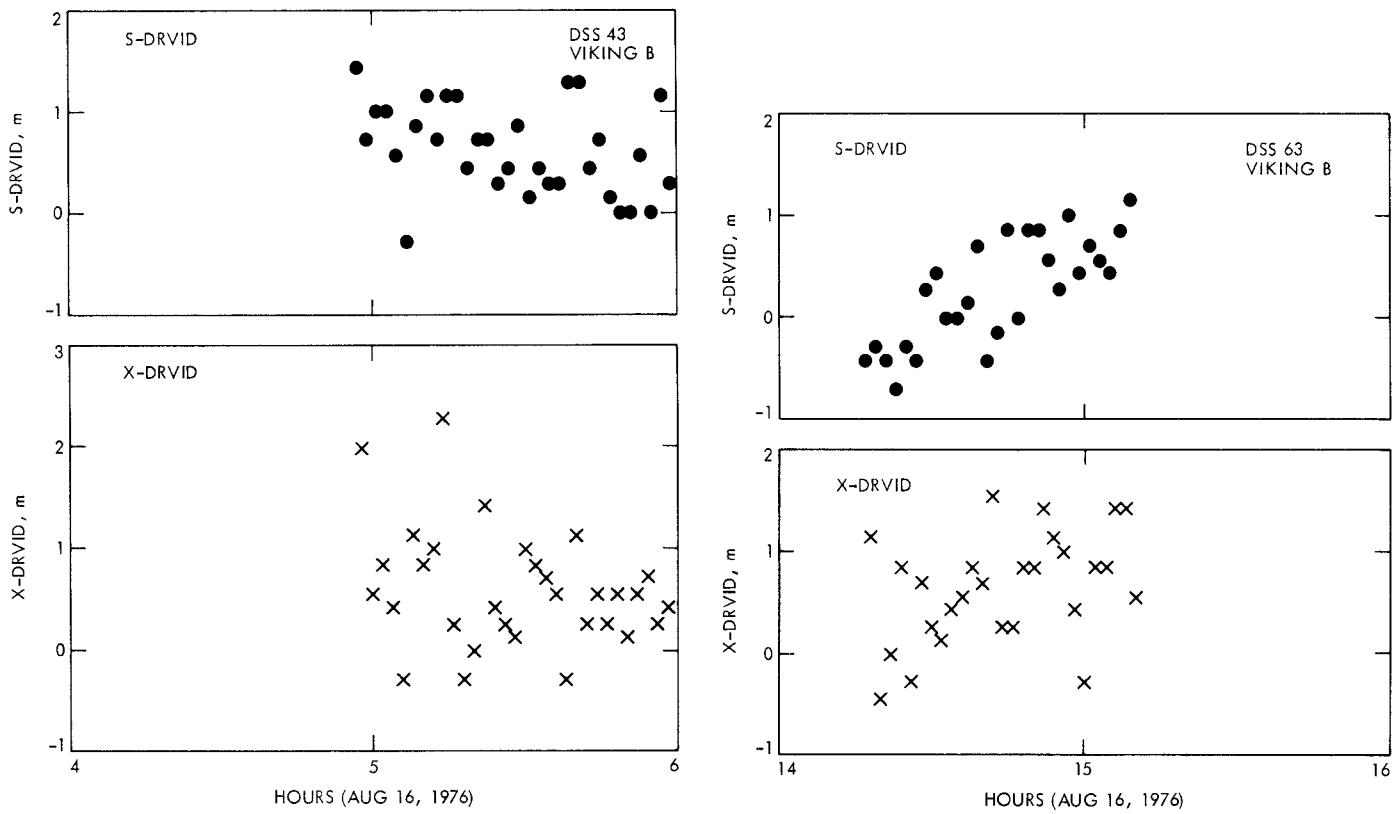

Fig. 10. S- and X-band DRVID

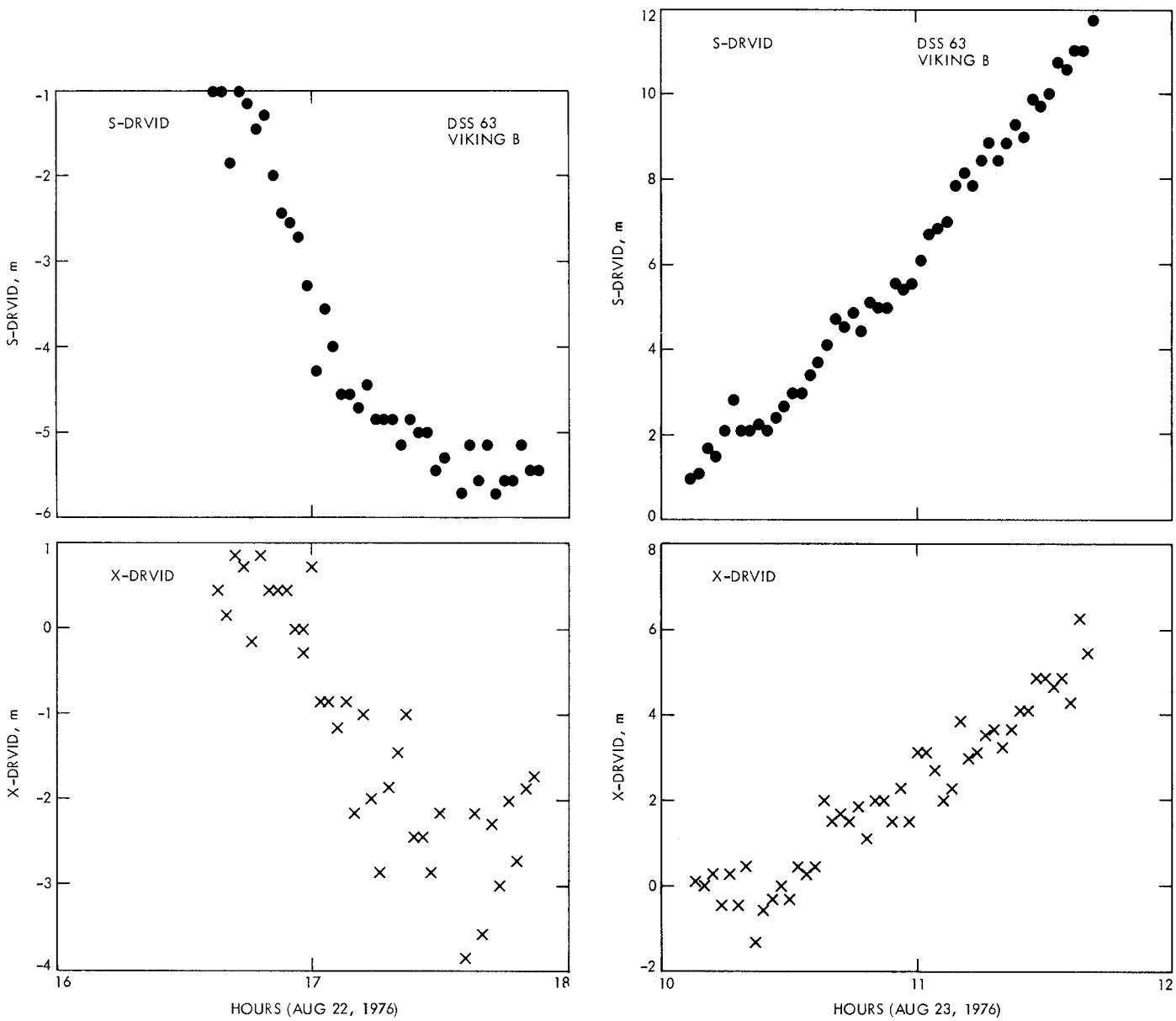
S-DRVID
DSS 63
VIKING B
S-DRVID, m
X-DRVID
X-DRVID, m
HOURS (AUG 22, 1976)
HOURS (AUG 23, 1976)

Fig. 10 (contd)

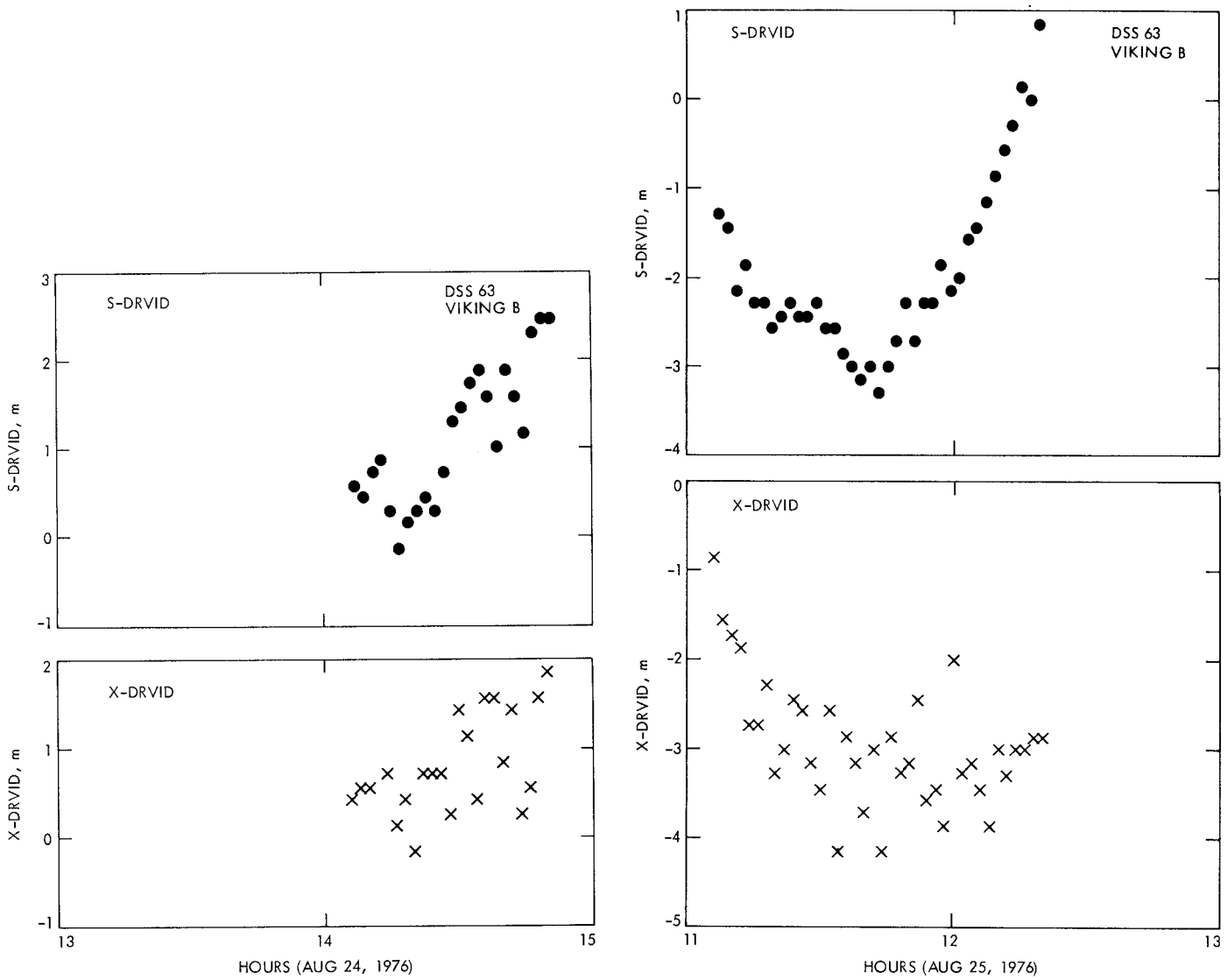
S-DRVID
DSS 63
VIKING B
S-DRVID, m
X-DRVID
X-DRVID, m
HOURS (AUG 24, 1976)
HOURS (AUG 25, 1976)

Fig. 10 (contd)

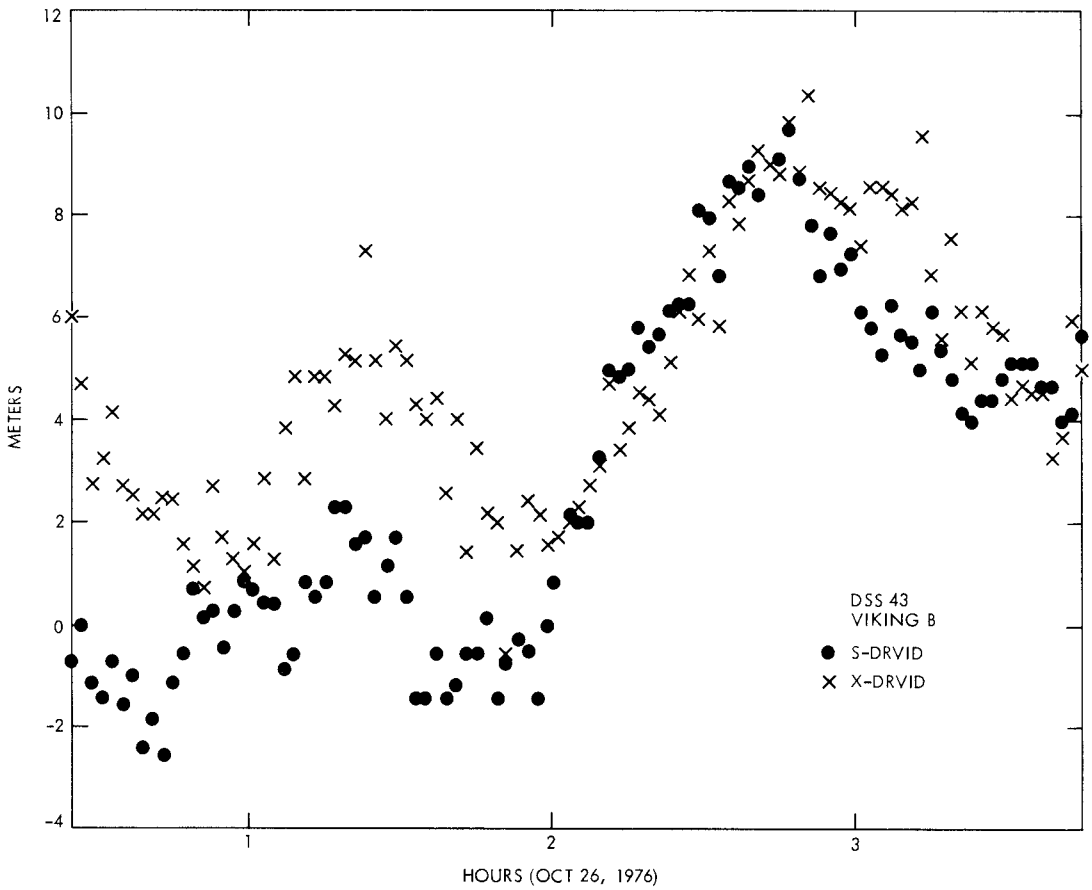
12
10
8
6
4
2
0
-2
-4
METERS
1
2
3
HOURS (OCT 26, 1976)
DSS 43
VIKING B
S-DRVID
X-DRVID

Fig. 10 (contd)

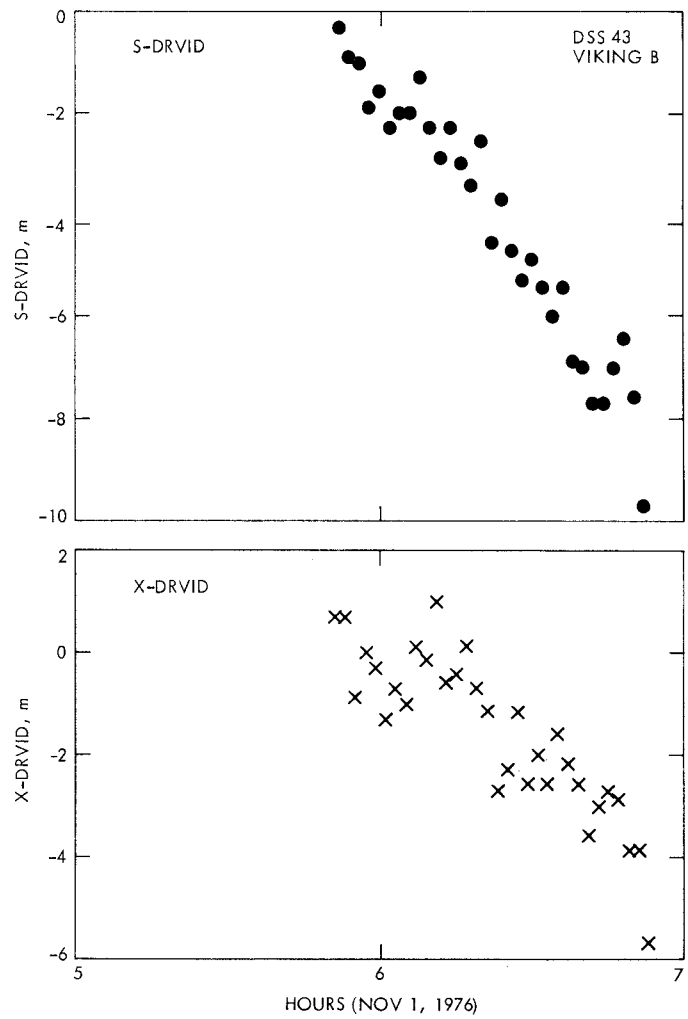
S-DRVID
DSS 43
VIKING B
S-DRVID, m
0
-2
-4
-6
-8
-10
X-DRVID
X-DRVID, m
2
0
-2
-4
-6
5
6
7
HOURS (NOV 1, 1976)

Fig. 10 (contd)

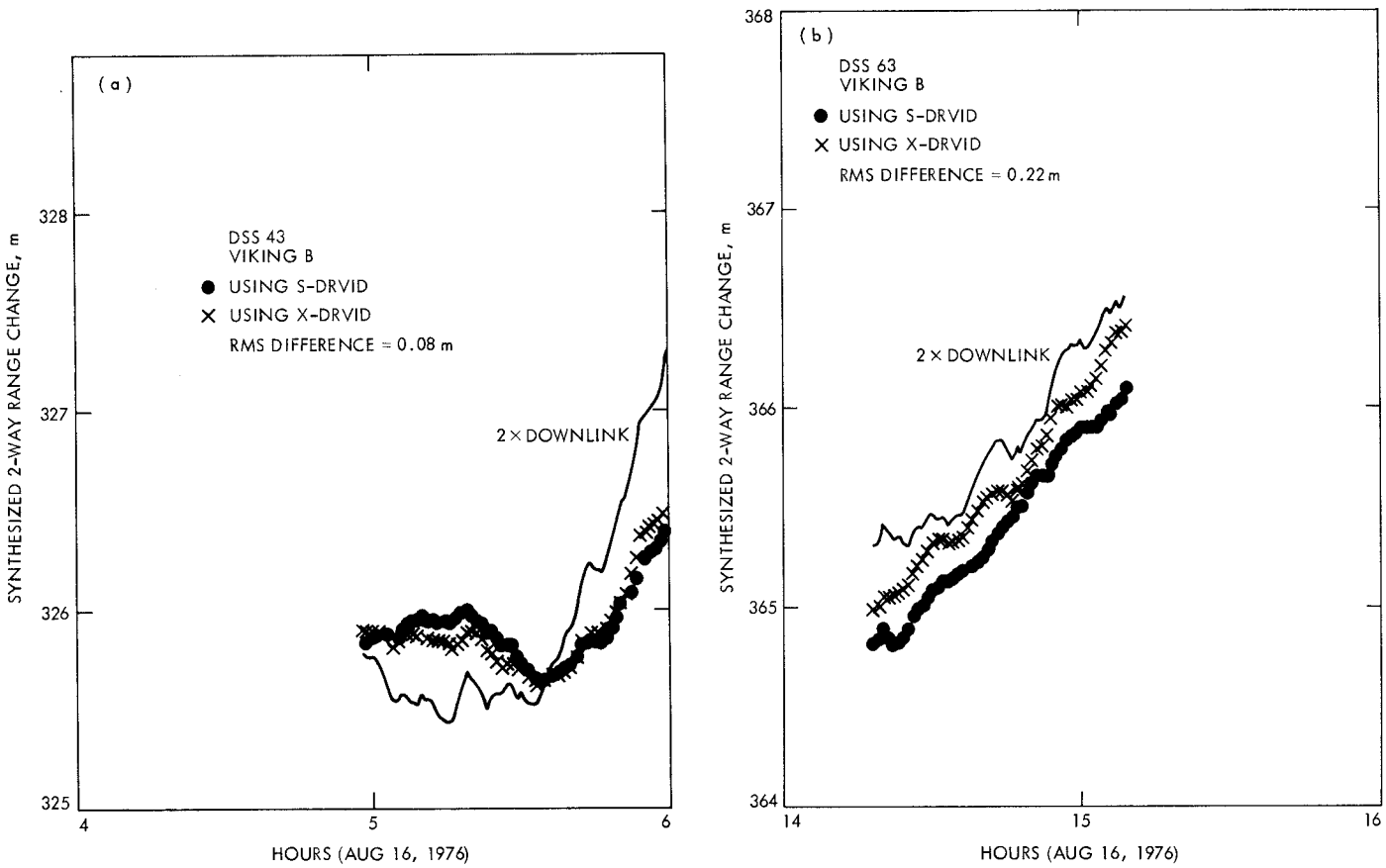

Fig. 11. Comparison of synthesized 2-way range changes and 2 x downlink range change

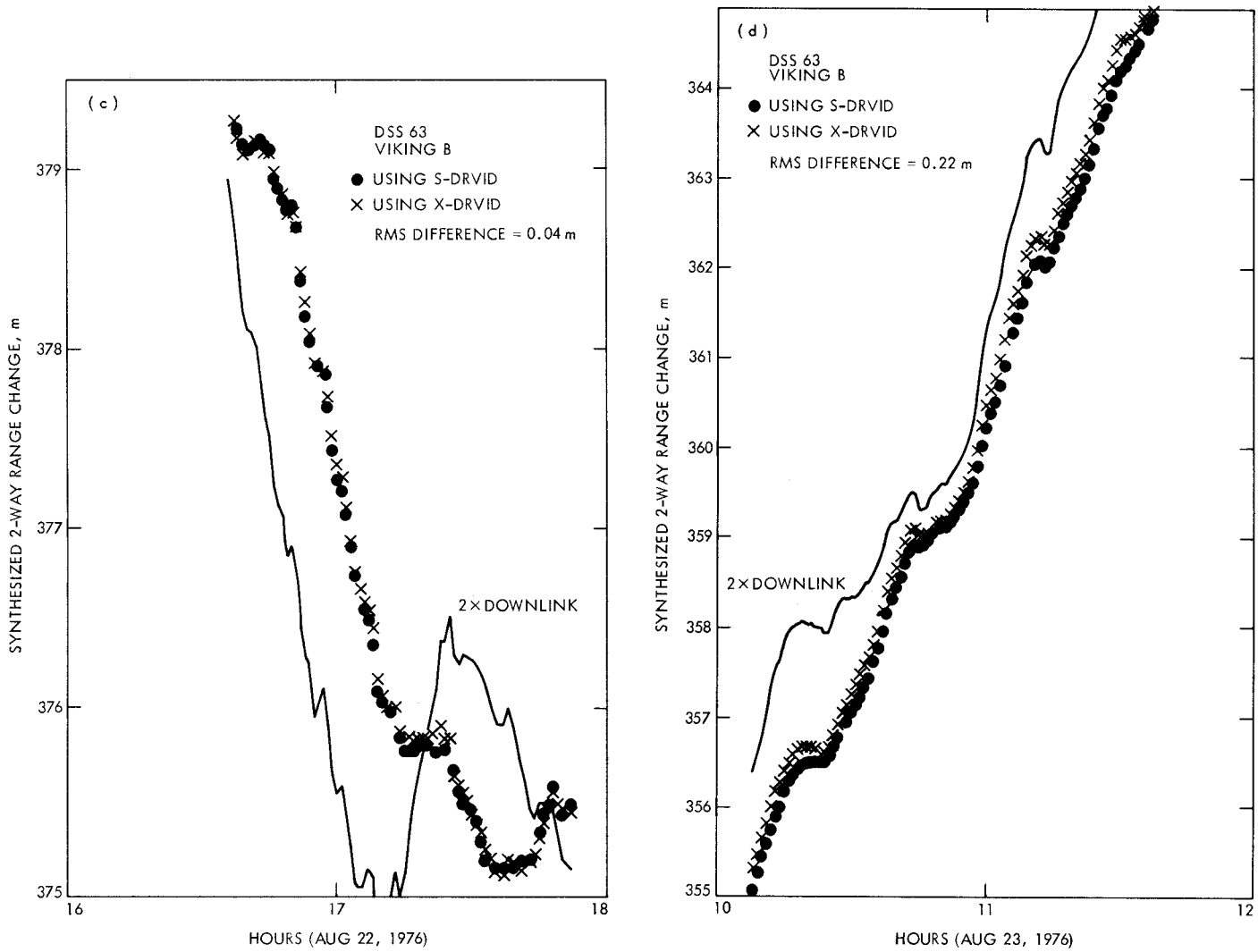
(c)
DSS 63
VIKING B
USING S-DRVID
USING X-DRVID
RMS DIFFERENCE = 0.04 m
2×DOWNLINK
SYNTHESIZED 2-WAY RANGE CHANGE, m
379
378
377
376
375
16
17
18
HOURS (AUG 22, 1976)
(d)
DSS 63
VIKING B
USING S-DRVID
USING X-DRVID
RMS DIFFERENCE = 0.22 m
2×DOWNLINK
SYNTHESIZED 2-WAY RANGE CHANGE, m
364
363
362
361
360
359
358
357
356
355
10
11
12
HOURS (AUG 23, 1976)

Fig. 11 (contd)

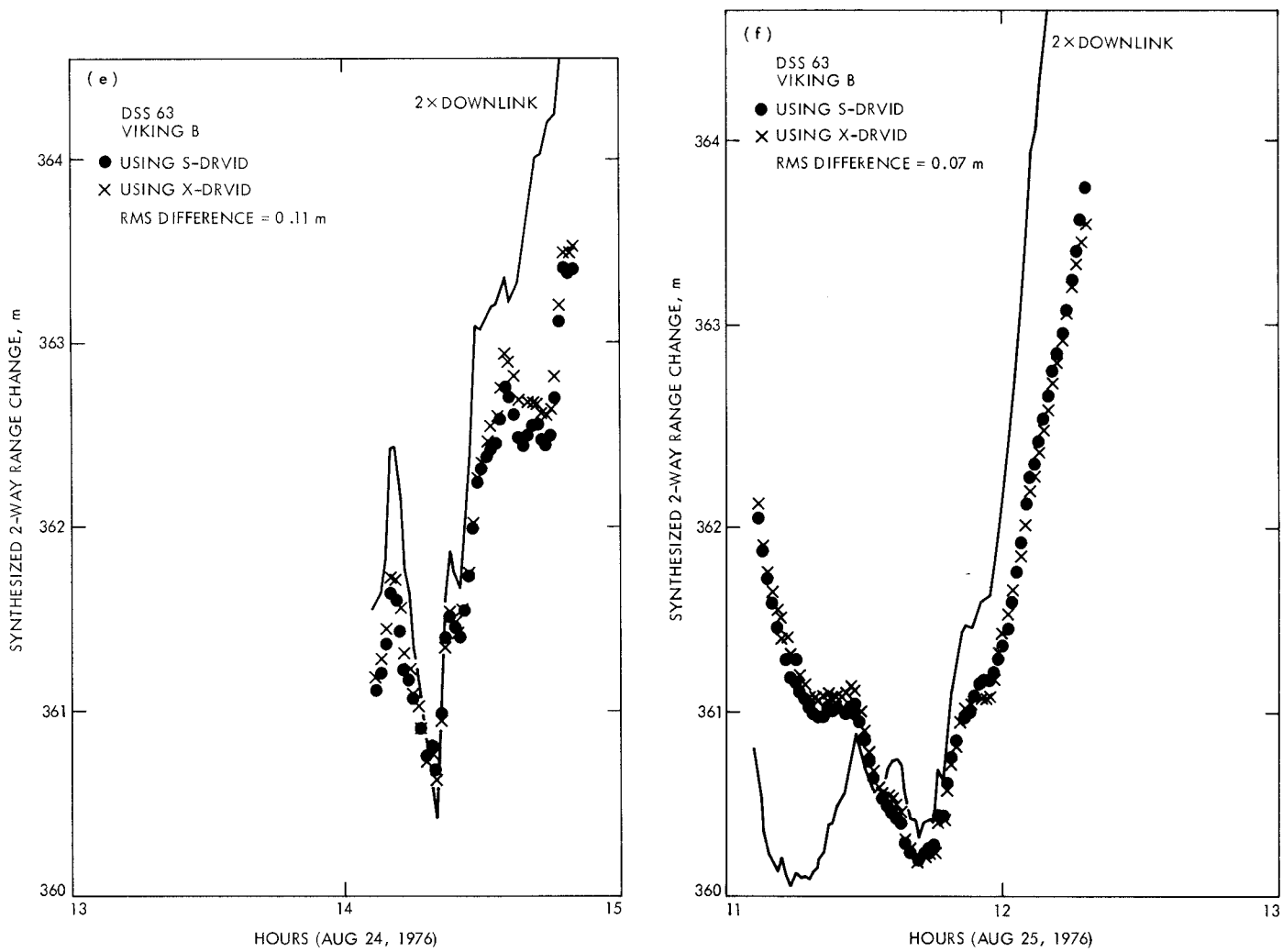
(e)
DSS 63
VIKING B
● USING S-DRVID
× USING X-DRVID
RMS DIFFERENCE = 0.11 m
2×DOWNLINK
SYNTHESIZED 2-WAY RANGE CHANGE, m
360
361
362
363
364
13
14
15
HOURS (AUG 24, 1976)
(f)
DSS 63
VIKING B
● USING S-DRVID
× USING X-DRVID
RMS DIFFERENCE = 0.07 m
2×DOWNLINK
SYNTHESIZED 2-WAY RANGE CHANGE, m
360
361
362
363
364
11
12
13
HOURS (AUG 25, 1976)

Fig. 11 (contd)

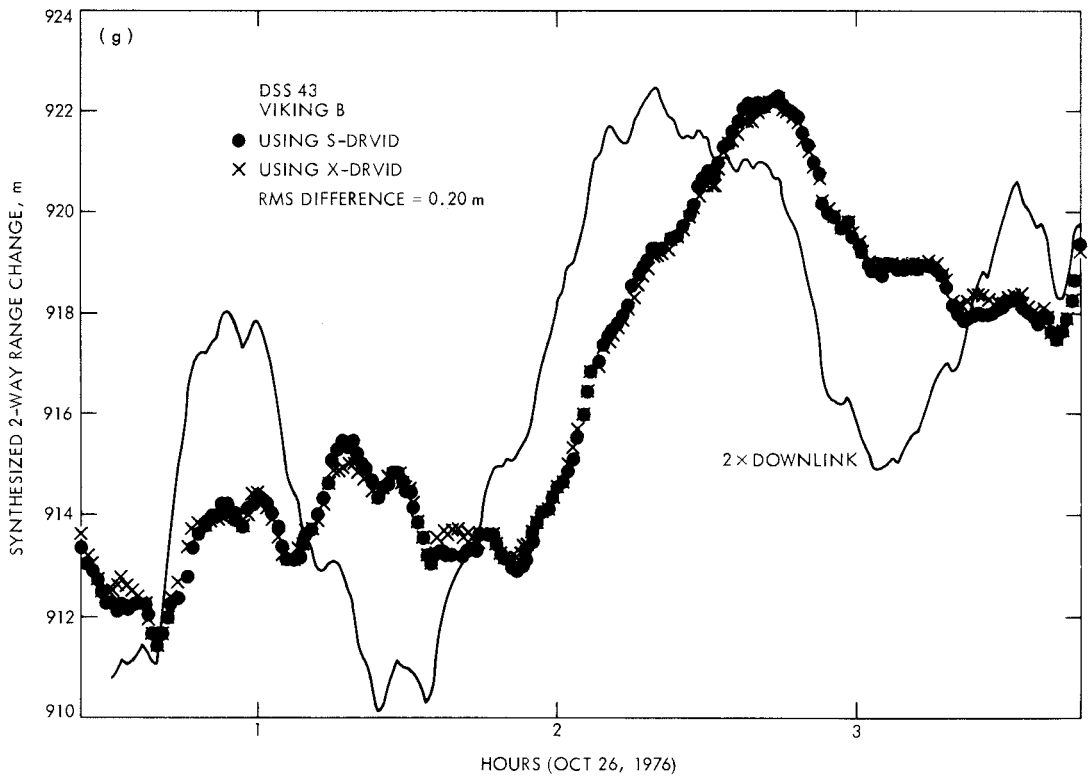
(g)
DSS 43
VIKING B
● USING S-DRVID
× USING X-DRVID
RMS DIFFERENCE = 0.20 m
2 × DOWNLINK
SYNTHESIZED 2-WAY RANGE CHANGE, m
924
922
920
918
916
914
912
910
1
2
3
HOURS (OCT 26, 1976)

Fig. 11 (contd)

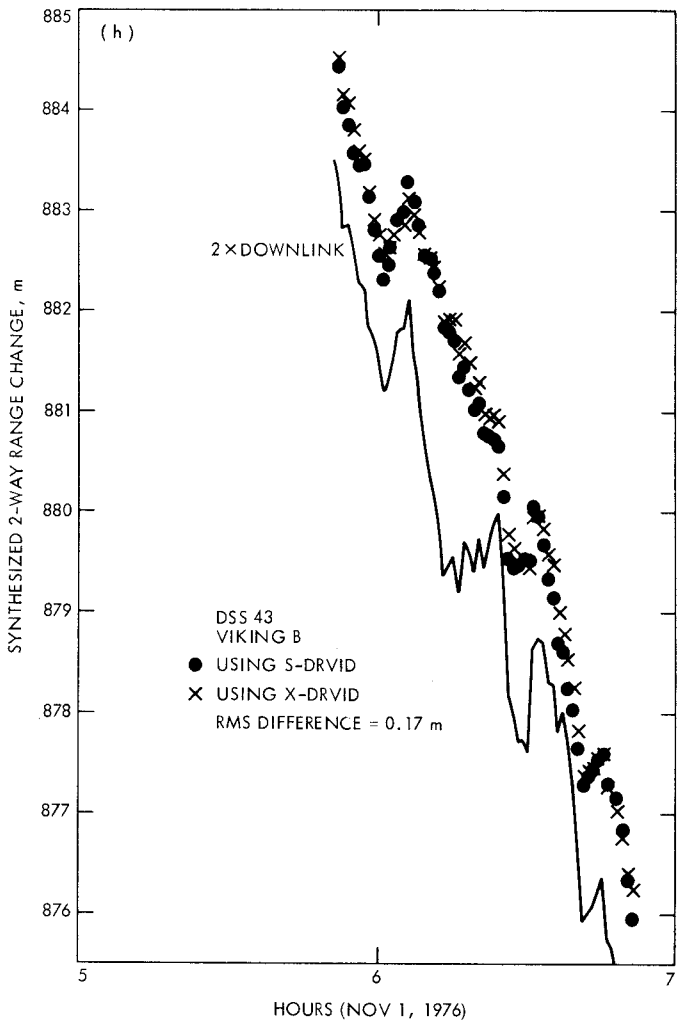
(h)
885
884
883
882
881
880
879
878
877
876
5
6
7
SYNTHESIZED 2-WAY RANGE CHANGE, m
HOURS (NOV 1, 1976)
2×DOWNLINK
DSS 43
VIKING B
● USING S-DRVID
× USING X-DRVID
RMS DIFFERENCE = 0.17 m

Fig. 11 (contd)

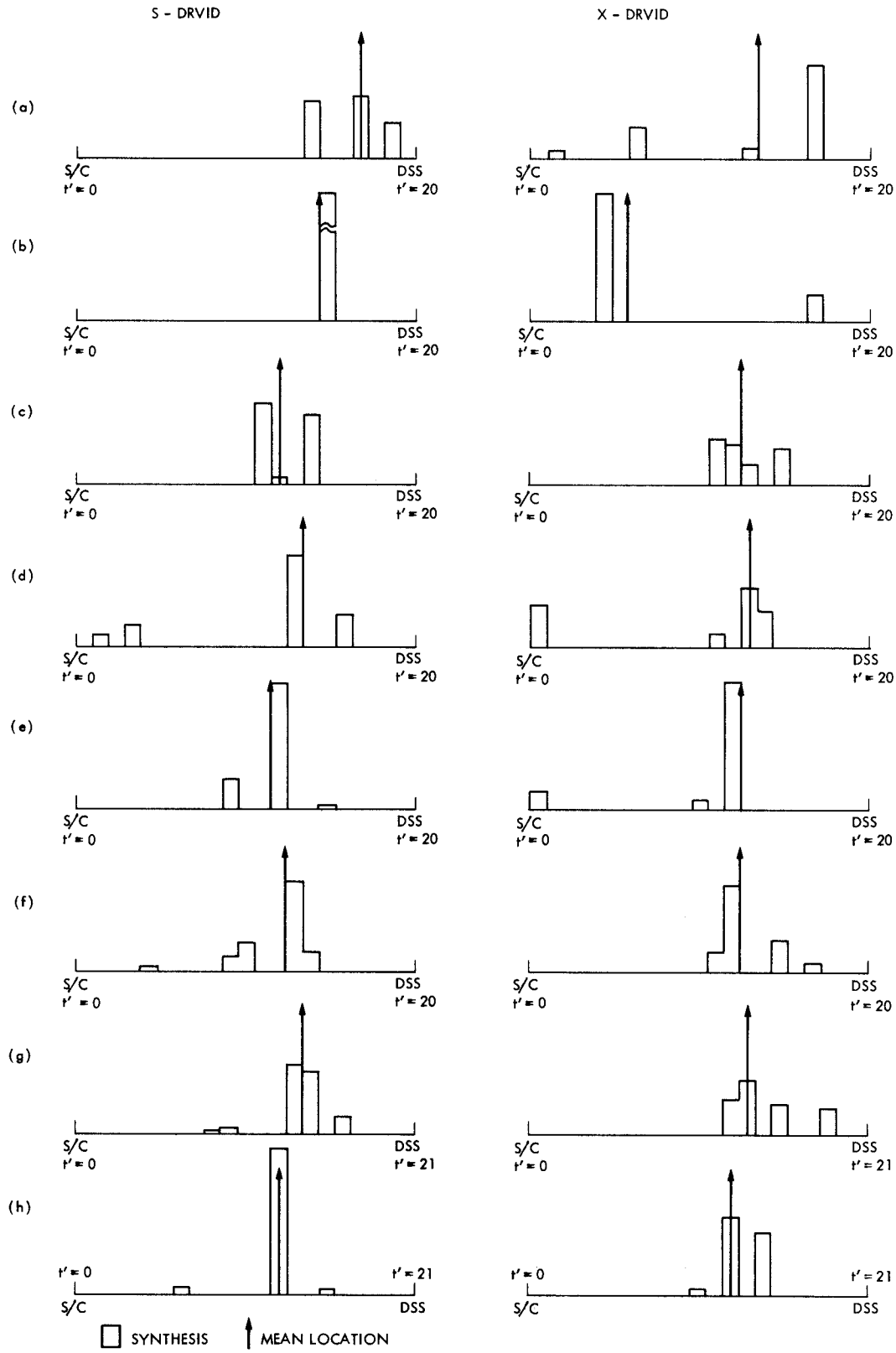

Fig. 12. Line-of-sight charged-particle relative distribution by synthesis and mean location by method of Ref. 3 (shown as arrows)